The Hubble constant and dark energy

Jeremy Mould

Centre for Astrophysics and Supercomputing, Swinburne University

ABSTRACT

The Hubble Constant measured from the anisotropy in the cosmic microwave background (CMB) is shown to be independent of small changes from the standard model of the redshift dependence of dark energy. Modifications of the Friedmann equation to include phantom power (w < –1), textures (w = –2/3) and curvature are considered, and constraints on these dark energy contributors from supernova observations are derived. Modified values for the density of matter inferred from cosmic density perturbations and from the CMB under these circumstances are also estimated, as exemplified by 2df and SDSS.

Subject headings: galaxies: distances and redshifts – cosmology: distance scale

1. Introduction

Turner (1999) coined the term dark energy to name the power source of the accelerating Universe (Garnavich et al. 1998; Perlmutter et al. 1999).

For the first time, there was a plausible, complete accounting of matter and energy in the Universe. Expressed as a fraction of the critical density there are: neutrinos, between 0.3% and 15%; stars, 0.5%; baryons (total), 5%; matter (total), 40%; smooth, dark energy, 60%; adding up to the critical density. This accounting is consistent with the inflationary prediction of a flat Universe and defines three dark-matter problems: Where are the dark baryons? What is the nonbaryonic dark matter? What is the nature of the dark energy? The leading candidate for the (optically) dark baryons is diffuse hot gas; the leading candidates for the nonbaryonic dark matter were slowly moving elementary particles left over from the earliest moments (cold dark matter), such as axions or neutralinos; the leading candidates for the dark energy involve fundamental physics and include a cosmological constant (vacuum energy), a rolling scalar field (quintessence), and light, frustrated topological defects.

Gooding et al. (1992) considered a Universe in which density fluctuations are produced in an initally smooth Universe by the ordering dynamics of scalar fields following a symmetry

breaking phase transition at the grand unified scale. Such transitions lead to the formation of an unstable topological defect known as "global texture."

Carroll [1] points out that for some purposes it is useful to pretend that the $-ka^{-2}R_0^{-2}$ term in the Friedmann equation represents an effective "energy density in curvature", and define $\rho_k -(3k/8\pi GR_0^2)a^{-2}$.

Caldwell (1999 astro-ph 8168) remarks that most observations are consistent with models right up to the w = –1 or cosmological constant limit, and so it is natural to ask what lies on the other side at w < –1. He termed this phantom energy.

In this paper we outline how a dark energy program will constrain these elements and, in particular, how they affect the measurement of the Hubble Constant by means of the anisotropy in the cosmic microwave background. Section 2 extends the Friedmann equation; §3 shows that supernova data are currently tolerant of small values of Ω_1 and Ω_2; §4 explores the degeneracies in CMB data; §5 examines how matter density experiments like 2dF (Peacock et al. 2001) are affected; §6 broadly explores the parameter space of Ω_n as it applies to SN and CMB data. Our conclusions are in the final section.

2. The Expansion Rate

An observer confronted with data like that in Figure 1 might respond by fitting a polynomial to the expansion rate as a function of redshift. But a physical equation already exists, namely the Friedmann equation.

$$(H/H_0)^2 = \Sigma_{-1}^4 a^{-n}\Omega_n = h^2 \tag{1}$$

From the point of view of fitting the data the observer might be surprised at the emphasis placed by physics on the higher order coefficients. This was not rectified until the discovery of dark energy, based on earlier versions of Figure 1 by the High z Supernova and Supernova Cosmology teams, although the zeroth order coefficient was considered and discarded by Einstein.

According to Gooding et al. (1992) the textures source term is

$$S_T = 4\pi G(\rho_T + 3P_T)\tau_*^2 a^2/(1 + a) \tag{2}$$

---

[1] (http://ned.ipac.caltech.edu/level5/Carroll2/Carroll2_1.html)

where τ_* is a time constant equal to $(8\pi G\rho_{eq}/3)^{-1/2}$ and the scale factor, a, is taken to be unity at the equality of matter and radiation. The quantities ρ_T and P_T are the density and pressure of textures respectively. The time constant is just the age of the Universe at equality. When a $>>$ 1, S scales like ρa, and textures will contribute to Ω_1. When a $<<$ 1, S scales like ρa^2, and textures will contribute to Ω_2.

The Ω coefficients are normalized by the Friedmann equation, so that

$$\Sigma_{n=-1}^{4}\Omega_n = 1 \tag{3}$$

where

$$n = 3(1 + w_n) \tag{4}$$

specifies the equation of state for matter and radiation components etc.

3. Fitting the Supernova Observations

The current supernova data (Conley et al. 2011) have been processed by Ned Wright and are shown in Figure 1. A value of $\Omega_k = 0.05$ does not violate the data. GRB data are also shown in Figure 1 (Schaefer 2006). The data are reproduced in Figure 2. Assuming $\Omega_{-1} = \Omega_2 = 0$, a value of $\Omega_1 = 0.1$ does not violate the data. The data are reproduced again in Figure 3, where we consider the case w = –4/3. Assuming $\Omega_1 = \Omega_2 = 0$, a value of $\Omega_{-1} = 0.1$ does not violate the data. Larger doses of textures, curvature, and phantom power would violate the data. We revisit these data to place firm constraints in §6.

4. Fitting the CMB

Some constraints on $\Omega_{\pm 1}$ and Ω_2 are imposed by the small scale anisotropy of the cosmic microwave background. Komatsu et al. (2009) deduced –0.0179 $<$ Ω_k $<$ 0.0081 (95% confidence).

We can derive similar constraints on Ω_n generally by requiring that the acoustic scale and shift parameter, R, (Komatsu et al. 2011) are conserved. We also invoke equation (3). For small values of the textures and curvature contributions, writing $\delta R = \Sigma \partial R/\partial \Omega_n \delta \Omega_n$ and a similar expression for the acoustic scale,

$$\Sigma_{n=0}^2 f_n \delta\Omega_n = 0; \qquad \delta\Omega_3 = 0; \qquad \Sigma_{n=0}^2 \delta\Omega_n = 0 \qquad (5)$$

where [2]

$$f_n = \int_0^z (1+z')^n h^{-3}(z')dz' \qquad (6)$$

The acoustic scale and shift parameter are conserved when introducing $\Omega_1 = \delta$ to the WMAP model provided $\delta\Omega_n = c_n\delta$ where c_n are coefficients of order unity and $c_1 = 1$, $c_3 = 0$, $c_0 = (f_1 - f_2)/(f_2 - f_0)$, and $c_2 = -(f_1 - f_0)/(f_2 - f_0)$ are computed in a simple numerical integration. Values are given in Table 1. For example, if $\Omega_1 = 0.1$, $\Omega_0 = 0.73 - 0.08 = 0.65$, and $\Omega_2 = -0.02$. Similar equations can be written for Ω_{-1} if we adopt $\Omega_1 = 0$. The change in the Hubble Constant deduced by WMAP is proportional to $\Sigma f_n c_n$ which is zero.

5. Density perturbations

Density perturbations in the Universe evolve as

$$\delta_{grow} \propto H \int_0^a da/\dot{a}^3 \qquad (7)$$

By requiring changes in δ_{grow} relative to those detected by 2dF and SDSS to be zero in response to $\delta\Omega_n$, we can follow the formalism of the previous section to obtain

$$\Sigma_{n=0}^3 g_n \delta\Omega_n = 0; \qquad \Sigma_{n=0}^3 \delta\Omega_n = 0 \qquad (8)$$

where

$$g_n = \int_{0.001}^1 a^{-(n+3)} h^{-5}(a)da \qquad (9)$$

.

Calculating the g_n values numerically (see Table 1), we find that the growth factor is conserved when $\delta\Omega_1$ and $\delta\Omega_2$ are introduced to the 2dF/SDSS model provided

$$\delta\Omega_3 = -0.127\delta\Omega_1 - 0.384\delta\Omega_2 \qquad (10)$$

.

---

[2]Equation (5) is simply derived for $dr_s/d\Omega_3 = 0$ and $dz_*/d\Omega_3 = 0$, but is also correct when the exact density dependence of the sound horizon, r_s, and CMB redshift, z_*, is included.

So perturbing the standard model by 0.1 in Ω_1, one would perturb the matter density measurement by only –0.01. And perturbing the standard model by 0.1 in Ω_k, one would perturb the density measurement by –0.04. This would be a significant change. Similar equations can be written for Ω_{-1} if we adopt $\Omega_1 = 0$.

6. Constraining $\Omega_{0,1,2}$ in a dark energy program

6.1. Combined SN and CMB constraints

From WMAP7 we formed the data vector (l_A, R, z_*) and calculated χ^2 for a full grid of values of Ω_n. For SNe χ^2 was calculated directly from the data shown in Figure 1. Marginalising over Ω_m, we can calculate probability in the $(\Omega_{\pm 1}, \Omega_2)$ plane given the SN data in Figure 1 and the WMAP 7 year data. The results are in Figures 4 and 5. We confirm what we found in section 4, that the Hubble Constant and the density of matter do not constrain these parameters.

6.2. The expansion rate at larger redshifts

A polynomial approach to dark energy in the Friedmann equation may actually lead to physical insights. Because unknown physical processes may be classified by how they scale with 1+z, they can at least be ranked by our approach.

Quintessence is beyond the scope of the present work.

$\Omega_{0,1,2}$ can be measured via experiments[3] to determine δh^2 at z = 2 and z = 3, where h is the dimensionless expansion rate, h(z).

Of course, our enthusiasm for polynomials should not obscure the real purpose of a dark energy program which is to determine the expansion as a function of redshift and the underlying physics, not simply an analytic form of the Friedmann equation.

---

[3]For example, $\Omega_2 = 72\delta_2 h^2 - 48\delta_1 h^2 - 0.3$, where $\delta_z h^2 = h^2(z) - h^2(1)$. If only one of these parameters is nonzero, e.g. Ω_2, then $\Omega_2 = 7.2\delta_2 h^2 - 0.17$ and it could be measured to 10% accuracy by a differential expansion rate experiment of similar measurement precision.

6.3. Dark Energy Surveys

Experiments such as the Dark Energy Survey (Frieman et al. 2005) and WiggleZ (Blake et al. 2011) are aimed at determination of the equation of state $P = \rho w$. Measurement of Ω_1 and Ω_0 are also within their scope (Komatsu et al. 2009; equation 80).

$$a^{3(1+w_{eff})} = \Omega_\Lambda/(\Omega_0 + \Omega_1/a) \tag{11}$$

For small z and $w_{eff} \approx -1$,

$$3w'_{eff}z = \Omega_1/\Omega_0 = 0 \text{ for } \Omega_1 = 0 \tag{12}$$

where $w' = dw/da$.

Coefficients in the Friedmann equation are related to w by equation (4) and are identified in Table 1.

Table 1: Equation of state components

Ω_n	n	w_n	c_n	f_n	$-g_n$
phantom	−1	−4/3	4.6	0.307	−0.401
vacuum	0	−1	−0.815	0.662	0.552
textures	1	−2/3	1	0.964	0.824
"curvature"	2	−1/3	−0.185	2.294	1.368
matter	3	0	0		2.677
radiation	4	+1/3			

The c,f,g coefficients have been evaluated at $\Omega_3 = 0.27$.

7. Conclusions

Our primary conclusion is that introducing Ω_1 or Ω_{-1} does not change WMAP values of H_0 or Ω_m . It is easy to show that this conclusion extends to phantom energy generally for w < −1 with $\Sigma a^{-n}\Omega_n + a^{-x}\Omega_x = h^2$ and x < 0. Using the supernova data alone, it is not possible to determine all the Ω's because of degeneracies. But in combination with CMB data, the degeneracies are broken. Second, we find that $\Omega_1 < 0.2$ and $\Omega_{-1} < 0.1$ with 95%

confidence. Stricter limits will follow from dark energy program. Third, $\Omega_2 \approx -0.2\Omega_1$ for $\Omega_1 \ll 1$. If $\Omega_2 = \epsilon$ (say, 10^{-6}) due to inflation, $\Omega_1 < 0.018/(f_1 - f_0) = 0.06$.

REFERENCES

Blake, C. et al. 2011, astro-ph 1104.2948

Conley, A. et al. 2011, ApJS, 192, 1

Eisenstein, D. et al. 2005, ApJ, 633, 560

Frieman, J. and The Dark Energy Survey 2005, BAAS, 36, 1462

Garnavich, P. et al. 1998, ApJ, 509, 74

Gooding, A. et al. 1992, ApJ, 393, 42

Komatsu, S. et al. 2009, ApJS, 180, 330

Komatsu, S. et al. 2011, ApJS, 192, 18

Peacock, J. et al. 2001, Nature, 410, 169

Perlmutter, S. et al. 1999, ApJ, 517, 565

Schaefer, B. 2007, ApJ, 660, 16

Turner, M. 1999, The Third Stromlo Symposium: The Galactic Halo, ASP Conference Series, 165, 431
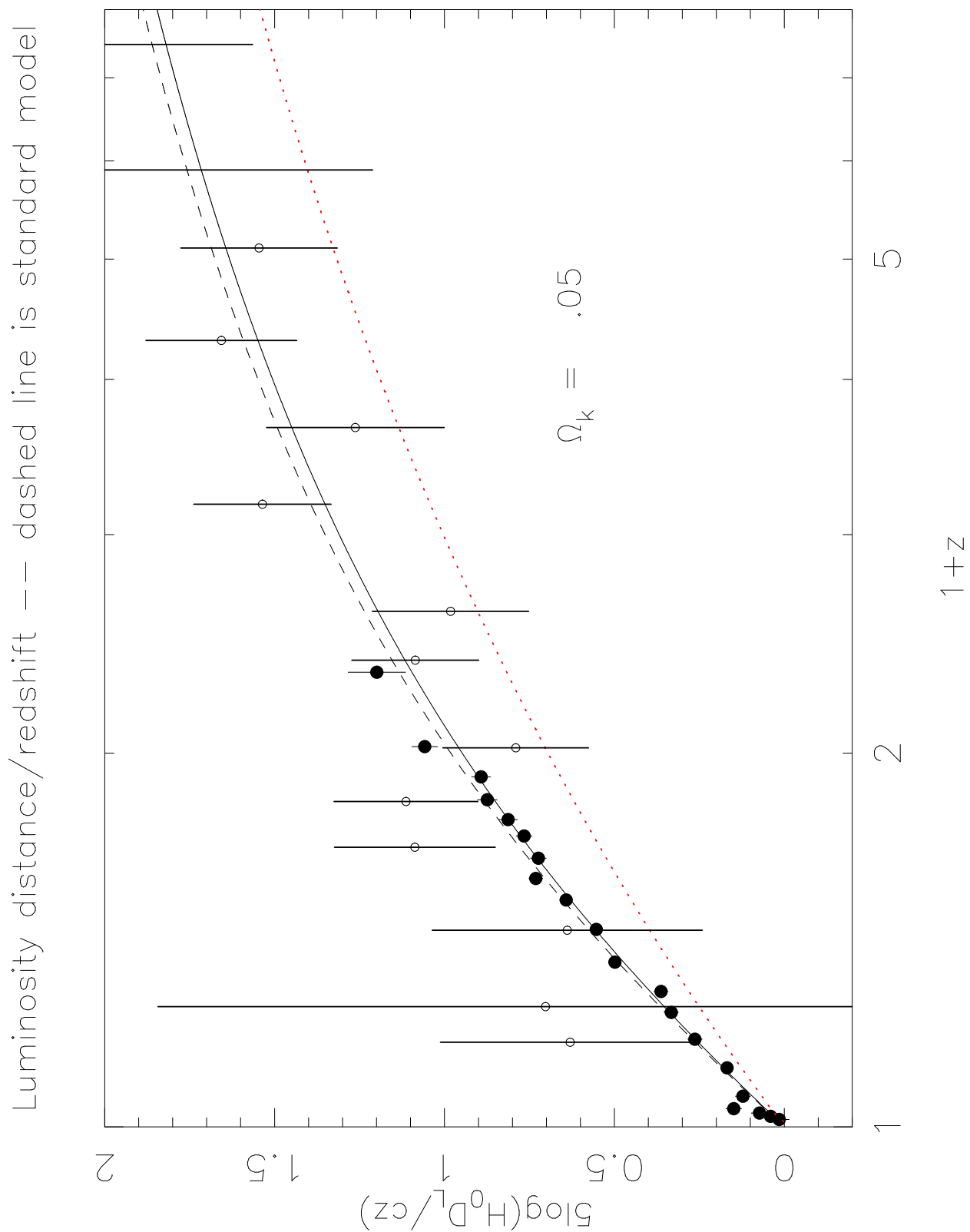
Fig. 1.— Curvature (solid curve for $\Omega_2 = 0.05$). The solid symbols are supernovae; the open symbols are GRBs. The standard model is the dashed curve. The red line dotted line shows that 0.5 violates the data.
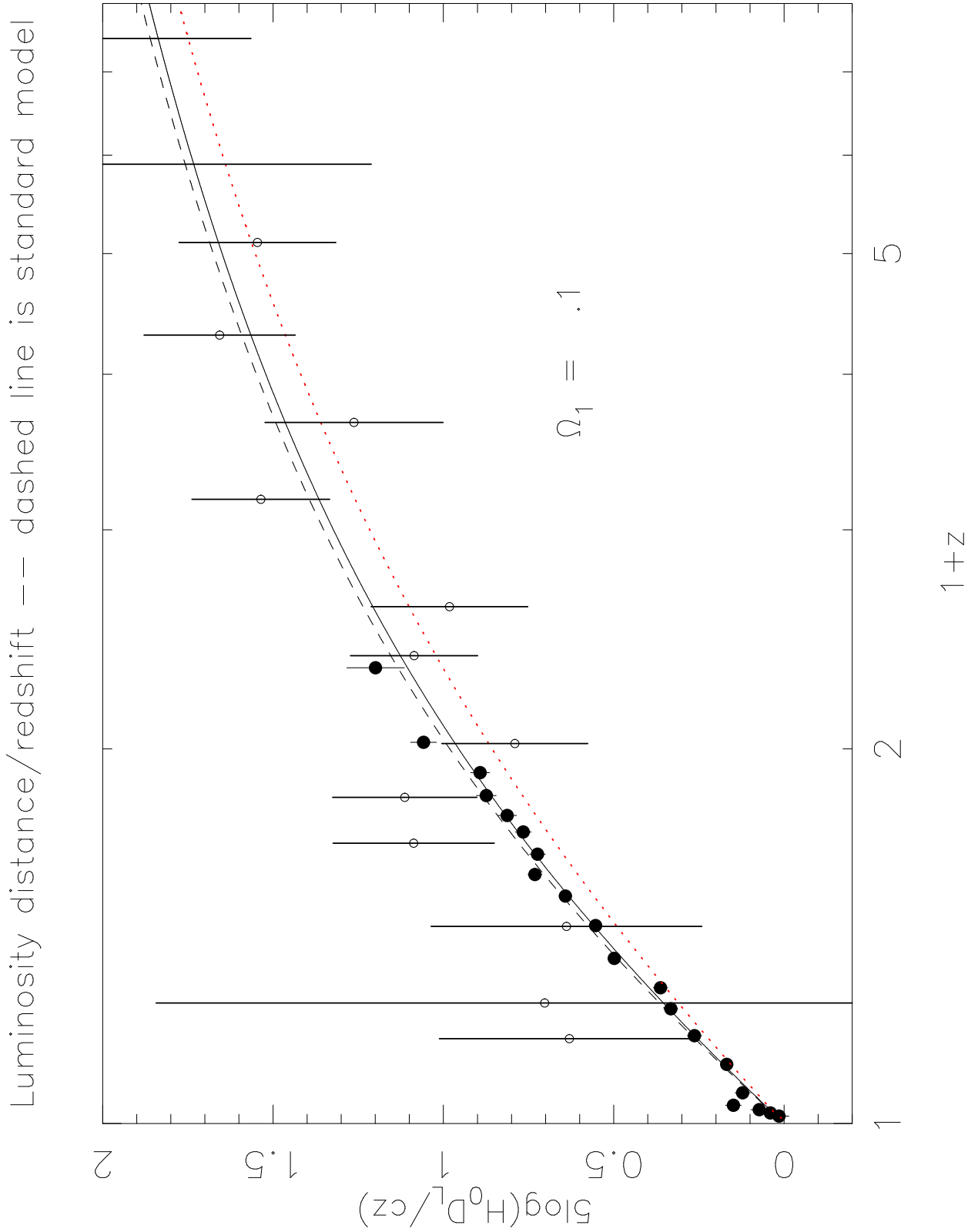
Fig. 2.— Textures (solid curve for $\Omega_1 = 0.1$). The standard model is the dashed curve. The red dotted line shows that 0.5 violates the data.
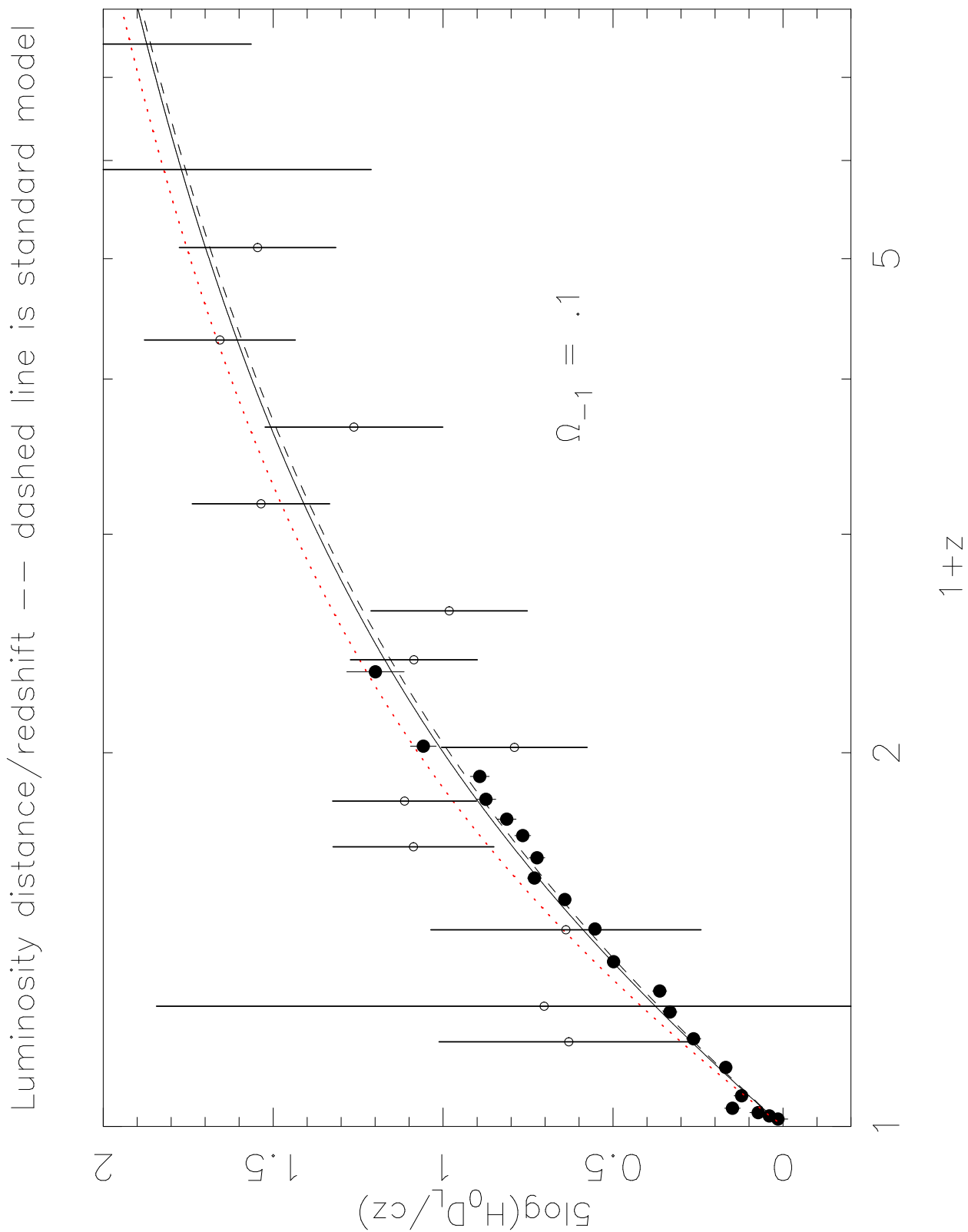
Fig. 3.— Phantom power (solid curve for $\Omega_{-1} = 0.1$). The standard model is the dashed curve. The red dotted line shows that 0.5 violates the data.
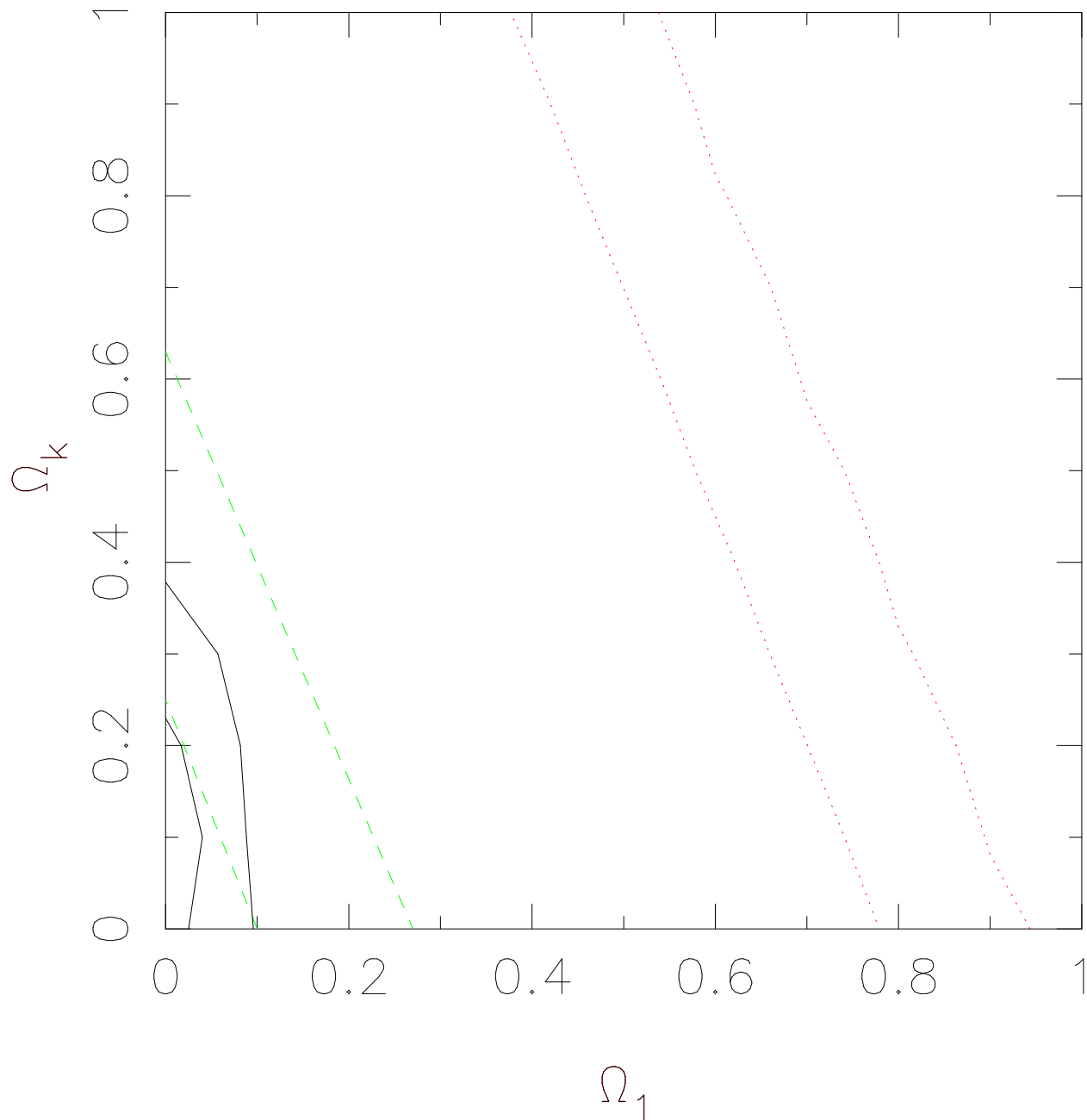
Fig. 4.— Probability contours (1σ and 2σ) for Ω_1 and Ω_2 given the WMAP7 CMB data and the supernova data in Figure 1. The SN contours are marked in red dots. The green dashed lines show the probability contours if a prior is added to the supernova constraint, namely $\Omega_3 = 0.273 \pm 0.025$ (Eisenstein et al. 2005) from SDSS. Constraints from Baryon Acoustic Oscillation experiments such as WiggleZ look like supernova constraints in this diagram, but are beyond the scope of the present paper.
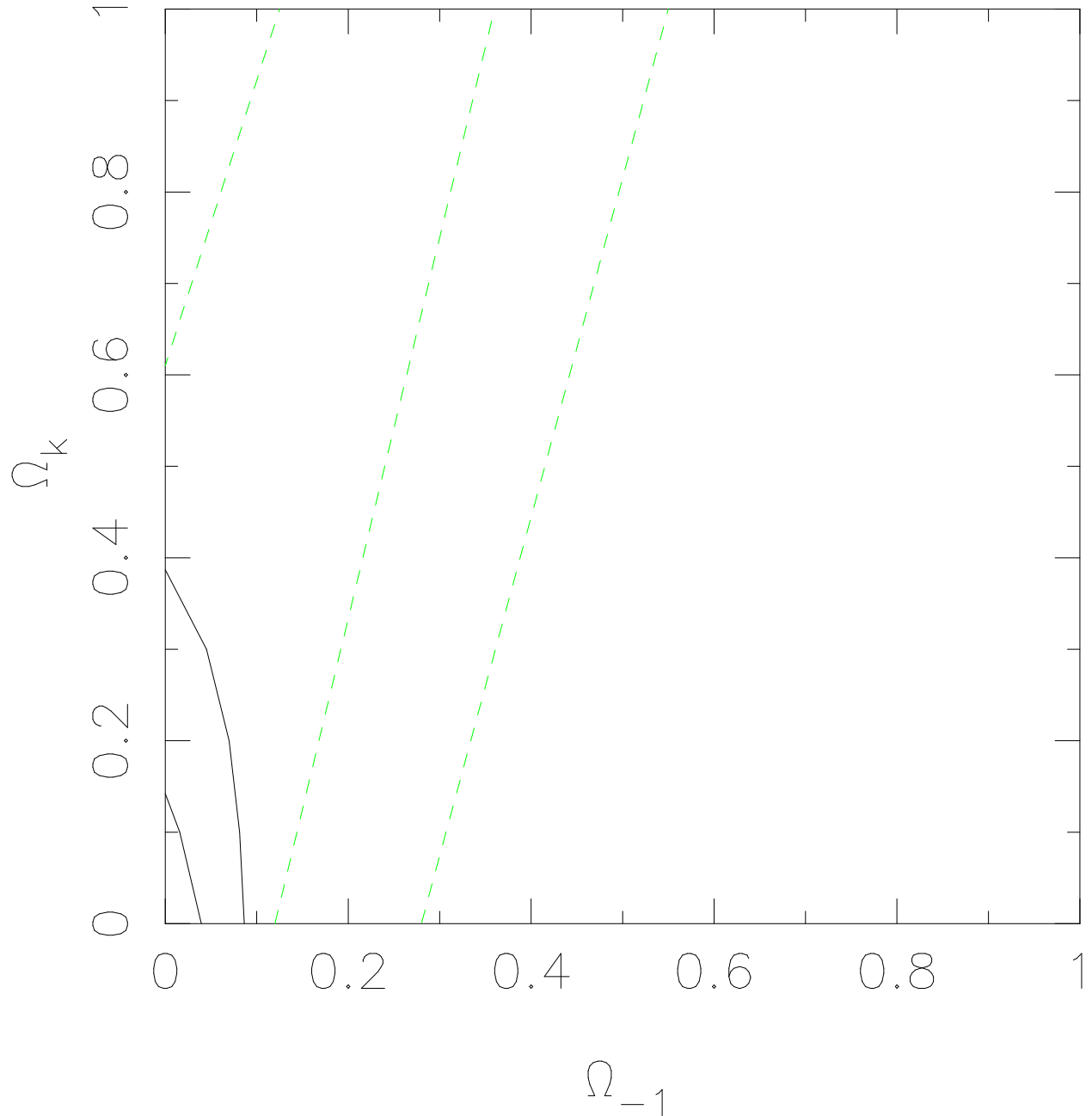
Fig. 5.— Probability contours (1σ and 2σ) for Ω_{-1} and Ω_2 given the WMAP7 CMB data and the supernova data in Figure 1. The green dashed lines show the probability contours if a prior is added to the supernova constraint, namely $\Omega_3 = 0.273 \pm 0.025$ (Eisenstein et al. 2005) from SDSS.